Thermal Noise Studies: Toward A Time-Domain Model of the ANITA Trigger

Amy Connolly, Stephen Hoover, David Saltzberg
(UCLA)
February 28, 2006

Abstract

We present studies of thermal noise as a first step toward modeling the ANITA trigger system using time-domain waveforms in the mainland simulation. We simulate time dependent noise in a slice of bandwidth similar to one of the ANITA channels and compare to measurements from a noise diode in the lab. We examine the behavior of the output of a simulated power integrator for different integration times and response functions, and show that an exponential distribution is only a good model of that output for a very specific set of parameters. With an exponential response function for the trigger diode, we achieve trigger rates similar to those reported from diode measurements, giving us confidence that we have developed the basic tools that we need to proceed to modeling the trigger response to Askaryan signals on thermal noise. We append a review of relevant features of thermal noise, and how to make comparisons between instantaneous and envelope detection measurements.

1 Motivation for Modeling Noise in the Time Domain

An understanding of noise is critical to simulating the behavior of the ANITA instrument. Ideally, we would like to simulate a trigger by adding a time-domain noise trace to a time-domain signal, and applying a model of a diode to the waveform. The latest version (v. 1.22) of the mainland ANITA Monte Carlo checks for a trigger by adding the peak instantaneous signal voltage to thermal noise in the frequency domain. The thermal noise is modeled by a Gaussian distribution. If the absolute value of the resulting voltage is greater than a preset threshold, the program registers a trigger. The actual system will trigger based on the output of a diode which integrates a time-domain signal. Inclusion in the Monte Carlo of a more realistic trigger process will improve the simulation's accuracy, and increase confidence in its results. We will also be able to produce a simulation of the actual data that will be recorded during the ANITA experiment. As a first step toward a full trigger simulation, we consider simulations and measurements of 200 MHz bandwidth noise such as will be encountered by each channel of ANITA, and compare to laboratory measurements. The work in this note is motivated by arguments and results from ANITA Note 68 [1].

2 How We Simulate Noise

Thermal noise is represented by the sum of a series of phasors with random phase, each corresponding to a different frequency [2, 3]. To construct simulated noise, we create a signal in the frequency domain in which all frequencies in band have unit amplitude and a phase chosen randomly from a flat distribution. (All frequencies are given unit amplitude because thermal noise is flat. True ANITA noise will not be exactly flat, but the exact form can be easily added to our simulations when data is available.) Each bin in frequency has its own phasor, and, because of the properties of the FFT, the bin size is determined from the duration of noise trace desired. The bin size is specified by $\Delta f = \frac{1}{T_N}$, where T_N is the trace duration. The time-domain signal is then obtained by taking an inverse Fourier transform of the frequency domain signal. All simulated noise traces described in this note were generated using a flat frequency spectrum from 550 MHz to 750 MHz, and sampled every 0.1 ns in the time domain.

3 Laboratory Measurements of Noise

In order to compare measured noise to simulated noise, we took measurements from a noise diode in the lab. The output of a Micronetics noise diode with ENR $\approx$ 21 dB was amplified by 33 dB, then passed through a high pass 550 MHz filter and a low pass 750 MHz filter. The 3 dB points of the resulting signal are at approximately 530 MHz and 750 MHz. The FFT of the noise signal, as taken by the scope, is shown in Figure 1. We recorded traces 50 μs long, sampled every 0.1 ns.

4 Characteristics of Passband Noise

We compare simulated noise to traces of measured noise recorded in the same band. Figure 2 has four typical sections of a simulated noise trace, and Figure 3 shows four sections of the same length of a measured noise trace. We generated the simulated noise using the method described in Section 2, and details of our noise measurements are given in Section 3. Both measured and simulated noise are sampled every 0.1 ns. The simulated noise can be seen to be similar in appearance to the measured noise. Note that the typical envelope period is on the order of 5 ns ($= \frac{1}{200\ \mathrm{MHz}}$), corresponding to the bandwidth of 200 MHz, and the oscillations within the envelope are around 1.5 ns ($\approx \frac{1}{650\ \mathrm{MHz}}$), corresponding to the center frequency of 650 MHz (as if it were a carrier).

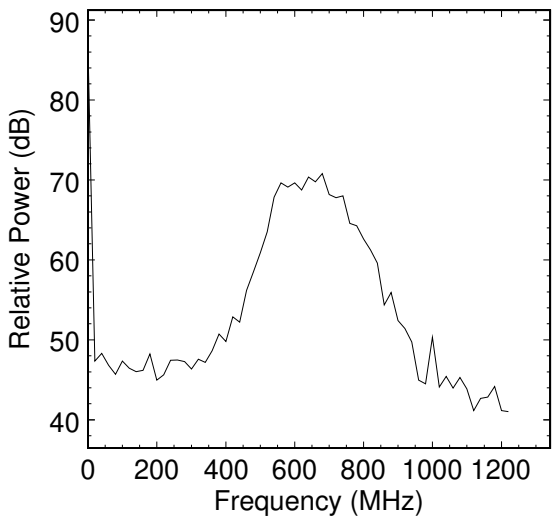

Figure 1: FFT of noise diode output passed through HP550 and LP750 filters.

4.1 Simulated Noise

We now examine the simulated noise more deeply to see if it has the characteristics we expect. We begin with the simplest case where all noise measurements are independent of each other. To do this, we create a large number of simulated noise traces, and take a single measurement from each trace. A different noise trace is used for each measurement in order to be absolutely certain that there are no correlations between successive measurements.

In Figure 4, we plot instantaneous uncorrelated voltages from the simulated noise traces. Using a fit provided by the ROOT libraries, we see that the distribution is Gaussian, with $\langle V \rangle = 0\ V$, and $\sigma = V_{\text{rms}} = 1\ V$. This is what we would expect; the distribution is Gaussian, as expected from the central limit theorem. It has a mean of 0 because the originating frequency distribution had no DC component. The RMS is 1, as expected when each bin in frequency has an amplitude of 1.

Figure 5 shows the distribution of envelope amplitudes from simulated noise. To create this distribution, we used an idealized envelope amplitude detector, as defined in the following equation:

$$\frac{a(t)}{\sigma} = \frac{\sqrt{2} \cdot \sqrt{\frac{1}{T} \cdot \sum_{i=0}^{N-1} (V(t - \Delta t \cdot i))^2 \Delta t}}{\sigma}. \tag{1}$$

With $\Delta t = \frac{T}{N}$, where Δt is the time step, T is the window of time where we perform the sum, and N is the number of discrete points over which we sum. In this case, we take

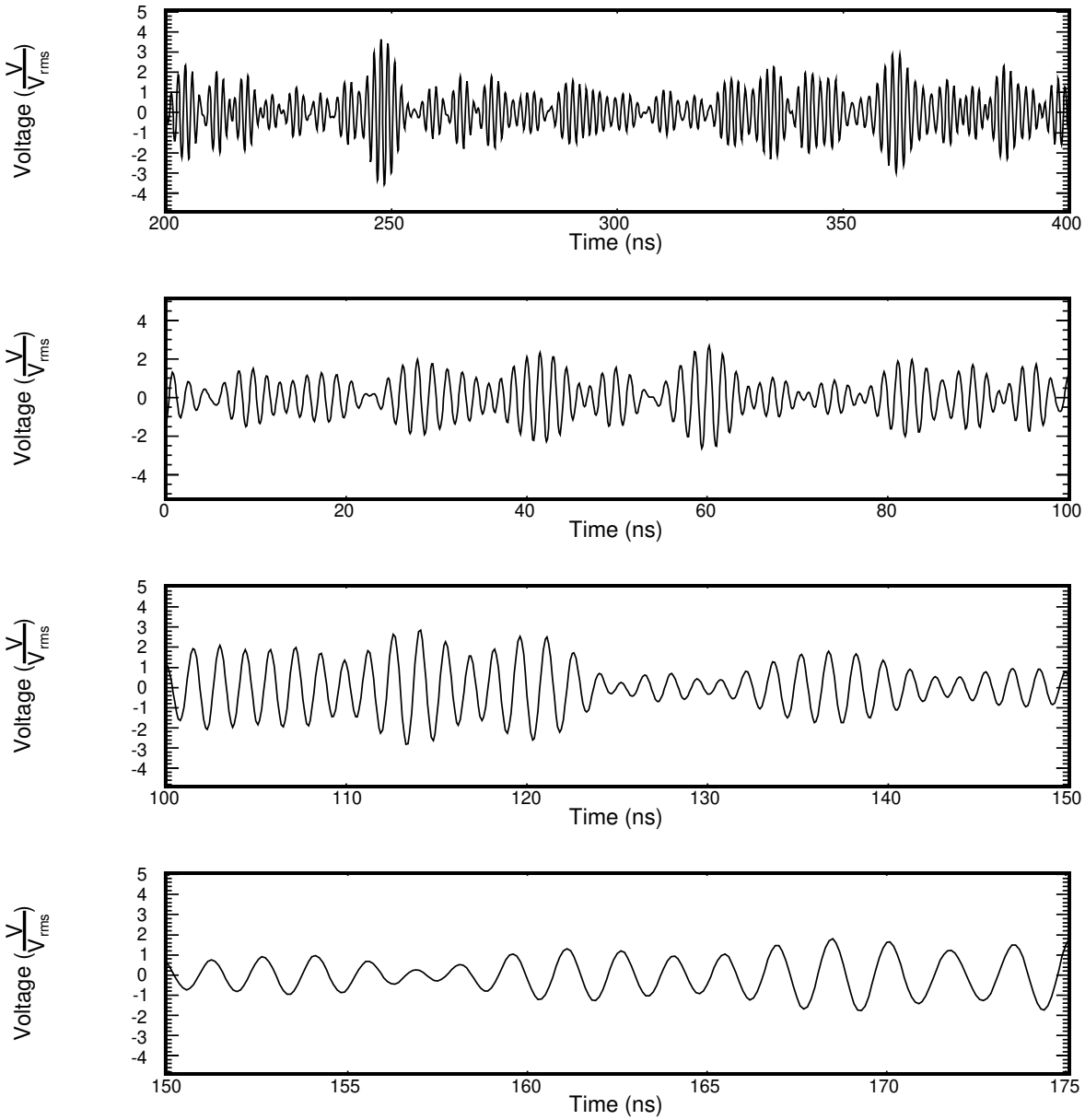

Figure 2: Simulated noise in a band from 550 to 750 MHz. Traces are of lengths 200 ns, 100 ns, 50 ns, and 25 ns, respectively.

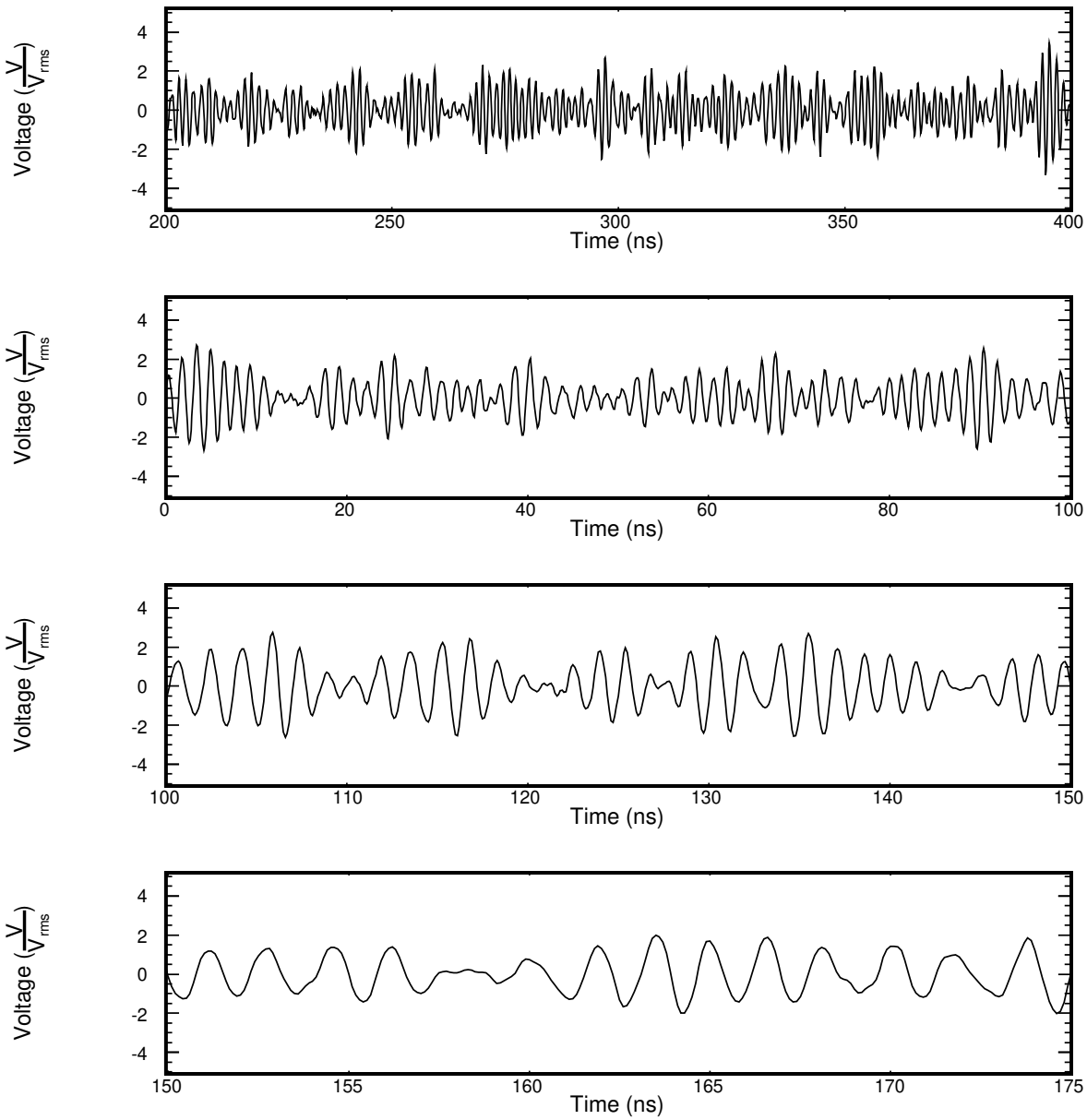

Figure 3: Measured noise in a band from 530 to 750 MHz. Traces are of lengths 200 ns, 100 ns, 50 ns, and 25 ns, respectively.

$\Delta t = 0.1$ ns and $T = 0.7$ ns. Here we choose T to be the length of one half-oscillation at the center frequency (0.7 ns $\approx \frac{1}{2} \cdot \frac{1}{650 \text{ MHz}}$). Note that we normalize by σ. We expect $a(t)$ to approximate the magnitude of the envelope at time t with these choice of parameters because the average voltage over one half-oscillation of the center frequency should be the peak of that oscillation divided by $\sqrt{2}$. Indeed, the distribution of $a(t)/\sigma$ in Figure 5 closely follows the overlaid Rayleigh distribution with $\sigma = 1$, as we expect for the envelope of noise with $\sigma = 1\ V$ [2, 3]. We note that another approximation of the envelope amplitude can be obtained by taking a linear interpolation between the two nearest peaks to the time of the measurement. The distribution obtained from this method is very similar to that given by $a(t)$ defined in Equation 1.

Finally, we model an idealized envelope power detector with simulated noise as its input and plot the result in Figure 6. The idealized envelope power detector is modeled using

$$\frac{I(t)}{\langle I \rangle} = \frac{\frac{2}{N} \cdot \sum_{i=1}^{N-1} (V(t - \Delta t \cdot i))^2 \Delta t}{2\sigma^2}, \tag{2}$$

where Δt is again given by $\Delta t = \frac{T}{N}$ with $T = 0.7$ ns and $\Delta t = 0.1$ ns. This expression can be obtained from Equation 1, using Equation 17. Note that we now normalize by $\langle I \rangle = 2\sigma^2$, as done by Goodman 4.2-8 [2]. The distribution of $I(t)/\langle I \rangle$ closely follows the overlaid exponential distribution (Figure 6) as we expect, following the discussion in Section A.2 and Reference [2]. Note also that the mean of the distribution is 1, indicating that our expression for $\langle I \rangle$ is correct.

4.2 Measured Noise

We now analyze the scope data in the same way as we did with the simulated noise in Section 4. As it is impractical to record 100,000 distinct scope measurements, the distributions all come from a single noise trace of duration 50 μs. Measurements are taken every 10 ns along the trace to ensure that the distributions are created from uncorrelated measurements. (A 10 ns shift suffices to obtain uncorrelated measurements, since the envelope size is 5 ns $= \frac{1}{200 \text{ MHz}}$). The scope data contains a DC offset not present in the simulated traces, and a different σ. For better comparison to simulated noise traces, the DC offset is removed by adding the same constant to all measured voltages. We also scale the amplitudes by multiplying all voltages by the same constant, such that the result has $\sigma = 1\ V$.

Plotting uncorrelated instantaneous voltages from the laboratory measurements gives us a Gaussian distribution (Figure 7), as we expect. Applying the idealized envelope amplitude detector described in Equation 1, we obtain a Rayleigh distribution (Figure 8), just as in the case of simulated noise. Finally, using the idealized envelope power detector described in Equation 2, we find an exponential distribution (Figure 9). We see, then, that our method for generating simulated noise produces distributions which agree both with

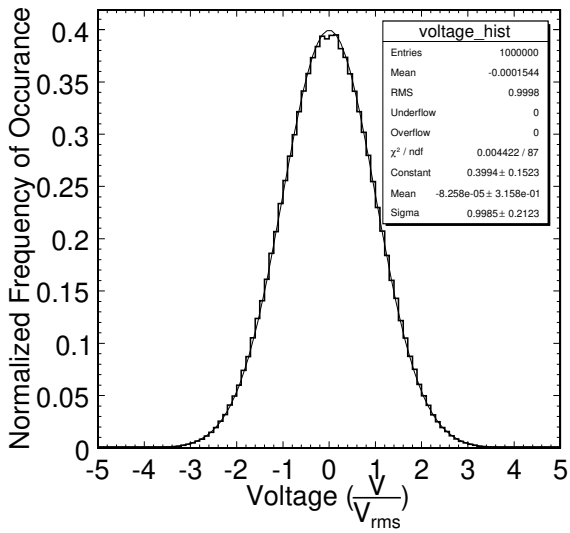

Figure 4: Distribution of uncorrelated voltages from a simulated noise trace. The overlaying line is a Gaussian fit, with parameters given in upper right.

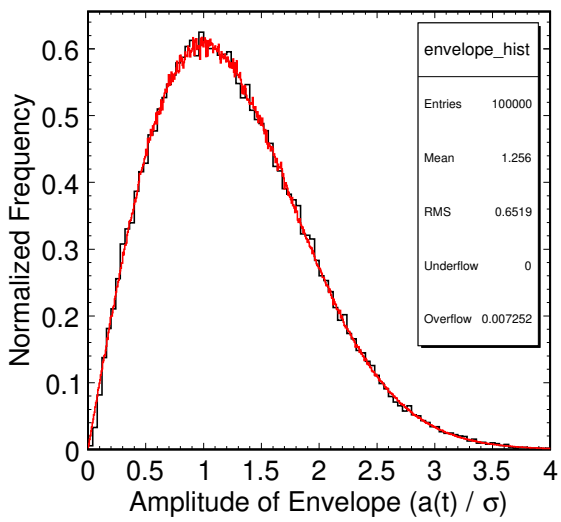

Figure 5: Distribution of randomly sampled uncorrelated envelope heights from a simulated noise trace, using Equation 1, $T = 0.7$ ns and $\Delta t = 0.1$ ns. The red line is a normalized Rayleigh distribution with $\sigma = 1$. (Not a fit.)

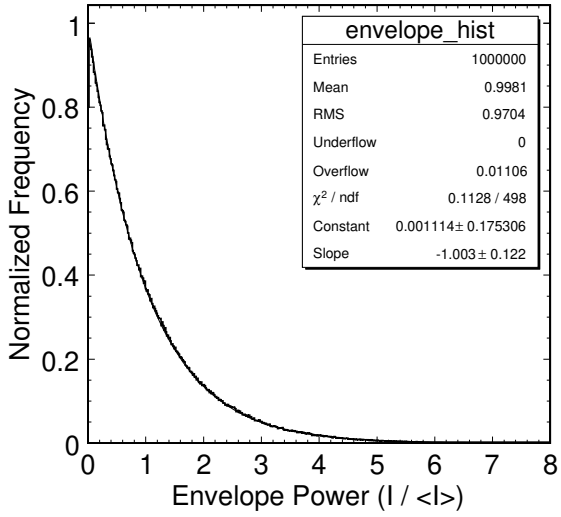

Figure 6: Distribution of randomly sampled uncorrelated instantaneous powers from simulated noise. The distribution is fit to an exponential, with parameters in the box in the upper right.

theoretical expectations, and with laboratory measurements of noise.

5 Noise Trigger Rates

Our ultimate goal is to incorporate this simulated noise into the ANITA Monte Carlo to allow for more realistic simulation of triggers. The true ANITA will trigger based on a diode reading of the incoming RF signal. The diode output is an integration of received power, with some response function. As a way to begin understanding the properties of such an integration, and to begin working up to a full diode simulation, we used the following sum on our noise traces:

$$\frac{F(t)}{\langle F(t)\rangle} = \frac{\frac{1}{N}\cdot\sum_{i=0}^{N-1}(V(t-\Delta t\cdot i))^2\cdot r(\Delta t\cdot i)\cdot\Delta t}{\langle F(t)\rangle}. \tag{3}$$

Note that, while in Equation 2 we had a defined expression for $\langle I\rangle$, there is no corresponding expression for $\langle F(t)\rangle$. We determine $\langle F(t)\rangle$ by plotting the full distribution of $F(t)$ and finding the average. Other than this, Equation 3 differs from Equation 2 only by the appearance of r(t), the "response function" which describes the weight given to each term in the sum. To date, we have experimented with two response functions. The first is a constant,

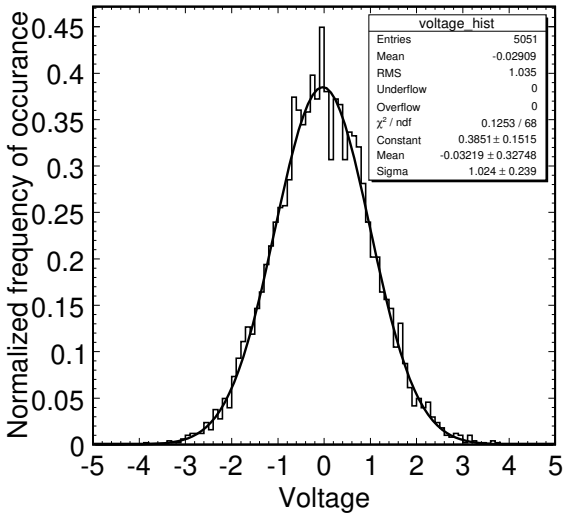

Figure 7: Distribution of uncorrelated voltages from scope data. Black line is a Gaussian fit, with parameters given in the box at upper right.

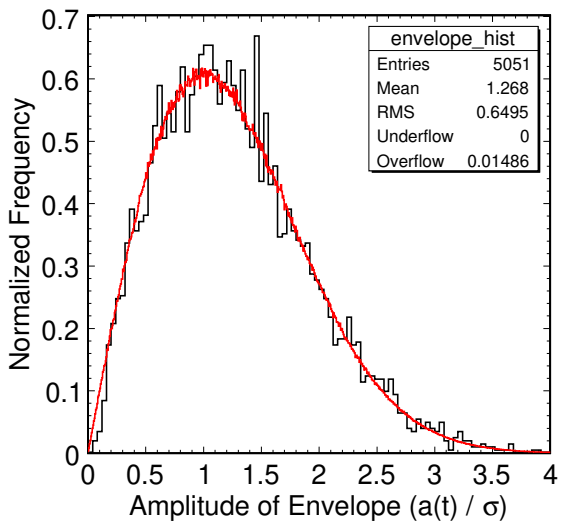

Figure 8: Distribution of uncorrelated envelope amplitudes from scope data. Red line is a normalized Rayleigh distribution with $\sigma = 1$. (Not a fit.)

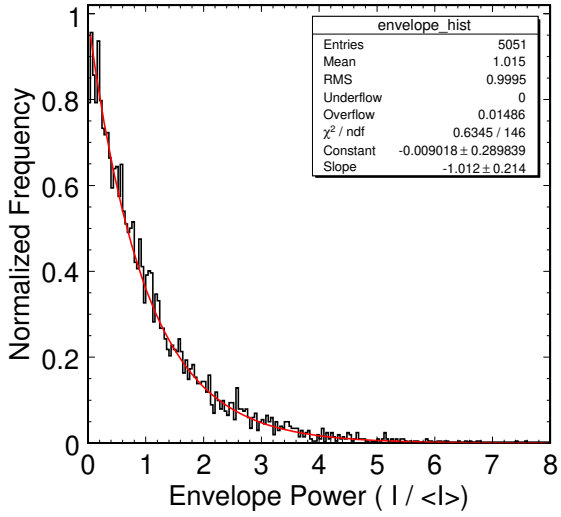

Figure 9: Distribution of uncorrelated envelope powers from scope data. Red line is an exponential fit, with parameters given in the box at upper right.

$r(t) = 1,\ 0 \leq t \leq T$ and $r(t) = 0$ at other times. This is referred to as a "square window". The second is $r(t) = \exp(-t/\tau),\ 0 \leq t \leq T$ and $r(t) = 0$ at other times, to simulate the response of an RC circuit with a time constant of τ. In this note, we take $\tau = 5$ ns. Note that when put in Equation 3, this response function de-weights earlier times exponentially.

To compare $F(t)/\langle F(t)\rangle$ for different response functions $r(t)$ and integration times T, we began by building up distributions of $F(t)/\langle F(t)\rangle$ on uncorrelated measurements. In Table 1, we give the value of $F(t)/\langle F(t)\rangle$ which is exceeded by 2.14% of the measurements. (A 2.14% probability corresponds to a 2.3 σ two-sided cut on a Gaussian distribution. This is the detection threshold currently being used in the ANITA Monte Carlos, and so is used here for reference.)

We begin by examining a square window of width $T = 0.7$ ns. We chose a width of 0.7 ns because it corresponds to approximately one half-cycle of voltage oscillation. The same integration width was used in Section 4 to measure envelope amplitude and power. The distribution of this $F(t)/\langle F(t)\rangle$ is shown in Figure 10. We find that a cut at 3.77 leaves us a 2.14% tail, as expected. The square window of width 0.7 ns gives exactly the idealized envelope power detector described in Equation 2, and so Figure 10 is an exponential distribution. In Section C, we saw that a cut of 3.7 ($\approx \frac{2.7^2}{2}$) on envelope power corresponds to a cut of 2.7 on the Rayleigh distribution of envelope amplitudes and $\approx 2.3\ \sigma$ on a Gaussian distribution. (Here we see that 3.77 is closer to the equivalent cut than 3.70.)

Next, we take a square window of width $T = 7$ ns. We chose 7 ns because we expect that the physical diode used in the ANITA trigger system will integrate over approximately this time. The diode will of course not have a response function $r(t) = 1,\ 0 \leq t \leq 7$ ns, but beginning with this simple weighting allows us to separate effects of integration time from effects related to the diode response. The distribution of this $F(t)/\langle F(t)\rangle$ is shown in Figure 11. We find that a cut of 2.86 leaves the desired tails. Figure 11 shows us why the cut has moved down — the tails of the distribution are lower than those from the response function with $T = 0.7$ ns. This is because we are now averaging the power over a longer time (≈ 5 oscillations of the center frequency, and > 1 oscillation of the envelope), and so we have far fewer extreme values. Note that, in fact, this trend continues as the integration time is increased (see Figure 13 and Figure 14, where we plot the result from a square window 70 ns wide and another 200 ns wide). As T increases, we sum over a greater number of envelope powers, each drawn from an exponential distribution. The distributions we obtain become narrower, and tend toward the Gaussian, by the central limit theorem. A Gaussian resulting from a large time windows should be centered at around $\frac{F(t)}{\langle F(t)\rangle} = \sigma = 1$, as can be seen in Figures 13 and 14.

Finally, we keep the 7 ns integration time, and include an exponential model of a diode response, $r(t) = \exp(\frac{-t}{\tau}),\ 0 \leq t \leq T$, with $\tau = 5$ ns and $T = 7$ ns. This gives the distribution of $F(t)/\langle F(t)\rangle$ shown in Figure 12. Now we find that the appropriate cut is at 1.60. The distribution is very similar to that produced by the 7 ns square window, but slightly wider. This is because earlier times are de-emphasized, and therefore $F(t)$ is more susceptible to extremes.

Up to now, we have been describing uncorrelated measurements. Next, we studied what sort of trigger rate we might get if we triggered off the output of each of the three integration functions described above using a trigger that takes measurements on the same trace in fine time steps. To find a trigger rate, the integration function is scanned across a noise trace, increasing time t by one step at a time. (Steps are $\Delta t = 0.1$ ns.) If the $F(t)/\langle F(t)\rangle$ exceeds a preset threshold, we count a trigger, and jump ahead by 50 ns, to represent the dead time after a trigger. We count the number of triggers in a given amount of time in order to find a trigger rate. Results are given in Table 2. Note that while the results in Table 1 are derived from uncorrelated measurements, we deal now with correlated measurements. One might naively expect that if we use cuts for each integration function such that the same percentage of measurements are above the cut for each distribution (i.e., 3.77 V/σ for the 0.7 ns square window, 2.86 V/σ for the 7.0 ns square window, etc.), we would obtain the same trigger rate. This is not the case, as our trigger rate depends on the number of peaks in $F(t)/\langle F(t)\rangle$ above threshold, not on the amount of time that $F(t)/\langle F(t)\rangle$ spends above threshold. A distribution with many short peaks will produce a greater trigger rate than a distribution with few long peaks. For examples of the output of $F(t)/\langle F(t)\rangle$ for different response functions acting on the same waveform, see Figures 15, 16, and 17.

The results in Table 2 illustrate this fact. The 0.7 ns square window gives the

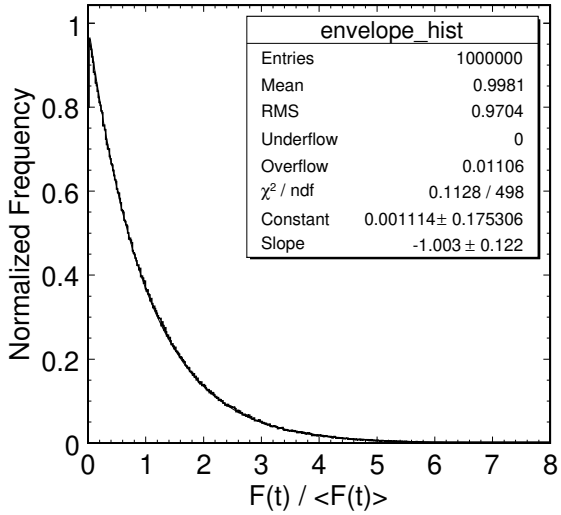

Figure 10: Distribution of $F(t)/\langle F(t)\rangle$ produced using a response function $r(t) = 1,\ 0 \leq t \leq T = 0.7$ ns. The distribution is fit to an exponential, with parameters in the box in the upper right.

highest trigger rate. It has the shortest integration time, and therefore is more prone to extremes than the other instances of $F(t)/\langle F(t)\rangle$. Because it changes more quickly, it has more peaks. The 7.0 ns square window averages over a larger time, and so has fewer peaks. The exponential response function integrates over more time than the 0.7 ns square window, and so varies more slowly (has a lesser trigger rate), but it response function has a narrower shape in time than the 7.0 ns square window does, and so varies more quickly (has a greater trigger rate) than the 7.0 ns square window.

A trigger rate of 2.0 MHz was suggested in [5] as a reasonable singles rate for the ANITA trigger. In Table 3, we show the thresholds required (in terms of $F(t)/\langle F(t)\rangle$) for a noise trigger rate of 2.0 MHz. In particular, we find that our exponential response function diode model ($r(t) = \exp(-t/5 \text{ ns}),\ 0 \leq \text{t} \leq 7$ ns) gives a noise trigger rate of 2.0 MHz when the threshold is set to 3.9. This matches well with the threshold on a physical diode in the lab found in [5], suggesting that our diode model is a reasonable first approximation of a physical diode.

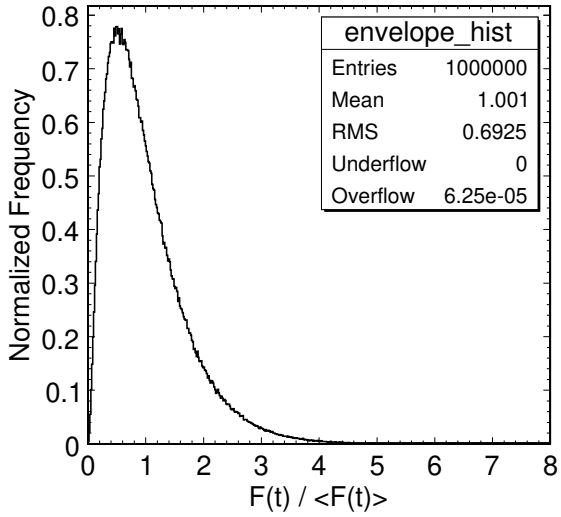

Figure 11: Distribution of $F(t)/\langle F(t)\rangle$ produced using a response function $r(t) = 1,\ 0 \leq t \leq T = 7$ ns. Note that the distribution is no longer exponential.

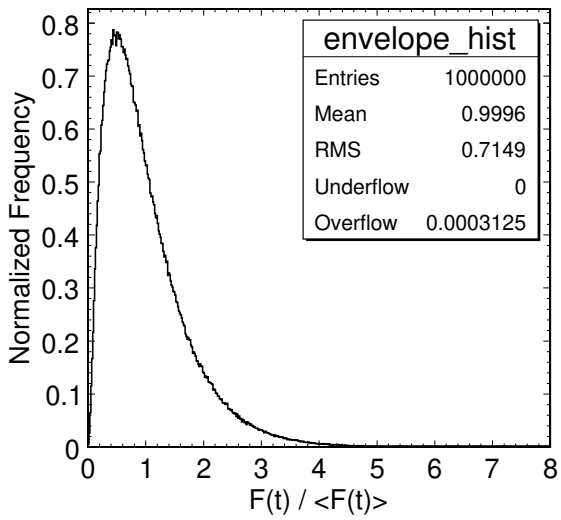

Figure 12: Distribution of $F(t)/\langle F(t)\rangle$ produced using a response function $r(t) = \exp(\frac{-t}{5\ \mathrm{ns}}),\ 0 \leq t \leq T = 7$ ns. Note that the distribution is no longer exponential.

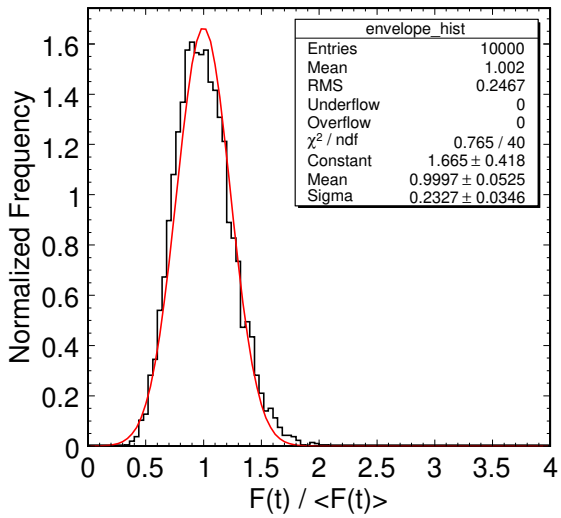

Figure 13: Distribution of $F(t)/\langle F(t)\rangle$ produced using a response function $r(t) = 1,\ 0 \leq t \leq T = 70$ ns. The red line is a Gaussian fit, with parameters given in the box at upper right.

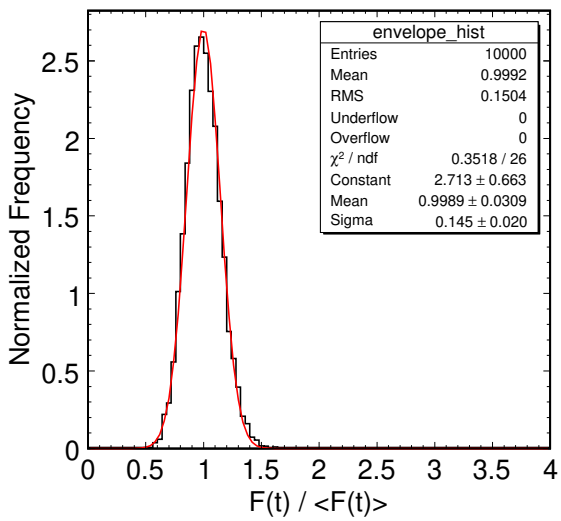

Figure 14: Distribution of $F(t)/\langle F(t)\rangle$ produced using a response function $r(t) = 1,\ 0 \leq t \leq T = 200$ ns. The red line is a Gaussian fit, with parameters given in the box at upper right.

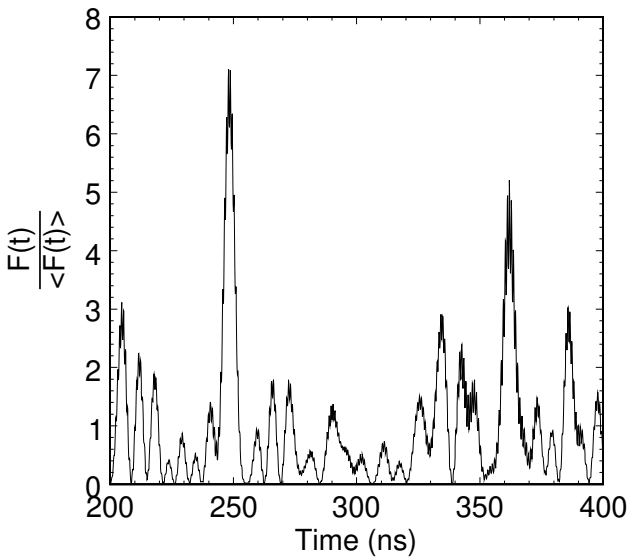

Figure 15: Value of $F(t)/\langle F(t)\rangle$ over a 200 ns span of a typical simulated noise trace, using $r(t) = 1,\ 0 \leq t \leq T = 0.7$ ns.

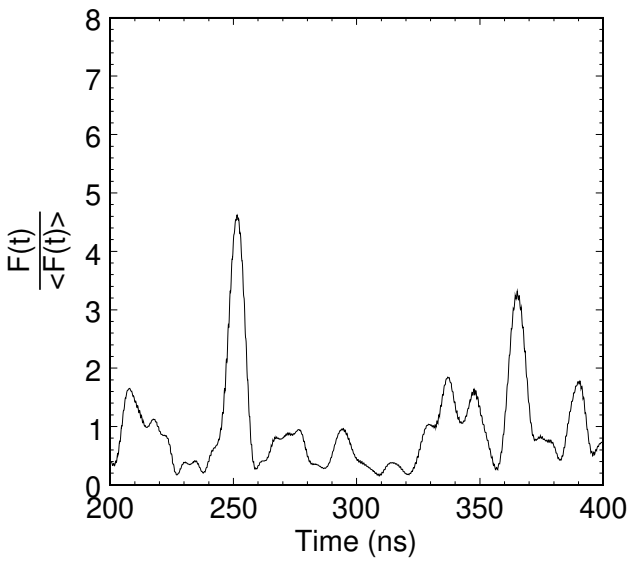

Figure 16: Value of $F(t)/\langle F(t)\rangle$ over a 200 ns span of a typical simulated noise trace (the same noise trace used in Figure 15), using $r(t) = 1,\ 0 \leq t \leq T = 7$ ns.

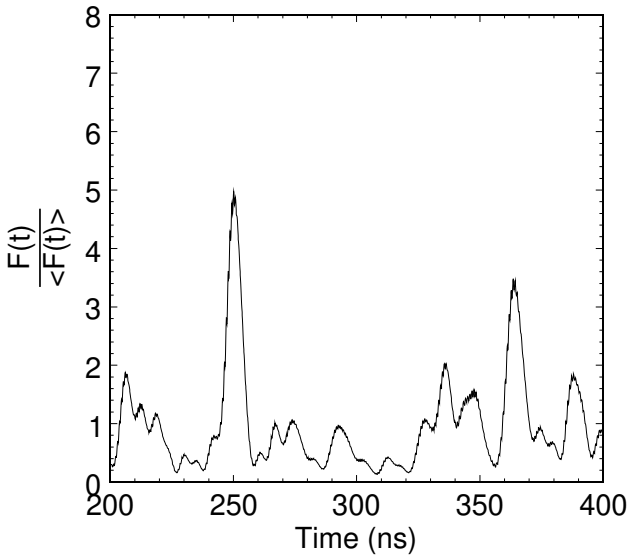

Figure 17: Value of $F(t)/\langle F(t)\rangle$ over a 200 ns span of a typical simulated noise trace (the same noise trace used in Figures 15 and 16), using $r(t) = \exp(\frac{-t}{5\ \mathrm{ns}}),\ 0 \leq t \leq T = 7$ ns.

Integration Type	Cut on $F(t)/\langle F(t)\rangle$ leaving a 2.14% tail
0.7 ns square	3.77 ($= \frac{2.7^2}{2}$)
7.0 ns square	2.86
7.0 ns exponential	2.94

Table 1: *Cuts on $F(t)/\langle F(t)\rangle$ distributions corresponding to a cut at 2.3 σ using the Gaussian formalism, i.e., leaving 2.14% of events in the tail.*

Integration Type	Trigger Threshold ($F(t)/\langle F(t)\rangle$)	Trigger Rate
0.7 ns square	3.77	7.7 MHz
7.0 ns square	2.86	4.8 MHz
7.0 ns exponential	2.94	5.5 MHz

Table 2: *Using thresholds found in Table 1, the resulting trigger rate.*

Integration Type	Trigger Rate	Trigger Threshold ($F(t)/\langle F(t)\rangle$)
0.7 ns square	2.0 MHz	5.8
7.0 ns square	2.0 MHz	3.6
7.0 ns exponential	2.0 MHz	3.9

Table 3: *Thresholds required to obtain a trigger rate of 2.0 MHz*

.

6 Conclusions

We have simulated thermal noise in the time domain and shown that its features are in good agreement with those of noise diode measurements in the laboratory. For the purpose of making those comparisons, we have shown what a perfect envelope detector looks like: it is an integrator that takes measurements with a flat response function and an integration time given by $\frac{1}{2f_0}$. We find that lengthening the integration time narrows the distribution of integrator outputs, and then a lower threshold gives the same probability for noise to exceed the threshold. An exponential response function makes an integrator behave like one with a slightly narrower integration window due to the drop in response for early times.

We then put an integrator into our trigger model. We found that the correlations bring about trigger rates that are lower than one might have naively expected from the cumulative distribution functions. By then lengthening the integration window, we find a lower trigger rate, even after lowering the thresholds to account for the lower probability of uncorrelated triggers as discussed in the previous section.

We find that if we use an exponential response function to model the trigger diode, we must set the threshold at 3.9 times the mean response to obtain a trigger rate of 2 MHz. This is identical to the threshold quoted in [5] for the same trigger rate. We also find that a threshold of 2.9 gives a trigger rate of 5.5 MHz, consistent with Figure 9 of [5] (although this point is slightly off the plot).

In this note, we have developed the basic tools that we need to model noise and the trigger diode response, and we are now ready to begin adding Askaryan pulses to the waveforms. The first order of business is to find the appropriate threshold on the Askaryan peak voltage that corresponds to the diode response of 3.9 and trigger rate of 2 MHz, since we have shown that the diode response is not properly modeled by the formalism that uses a Rayleigh (Rician) distributions to model the noise (noise + signal). There are competing effects that might pull the threshold in either direction: the long integration window allows for lower thresholds with regard to trigger rates, but they also act to suppress the signal compared to noise, so a stronger signal would be required to trigger the system. We ultimately plan to use a full simulation of a time-domain noise, signal, and trigger in the ANITA Monte Carlo.

A The Relationship Between a Cut in Voltage and a Cut in Power

A.1 Instantaneous Noise Voltage Follows a Gaussian Distribution

Knowing that a correct treatment of noise is derived from Rician distributions and proper modeling of the trigger diode, we use the simple Gaussian treatment of noise voltage for the purpose of this discussion about ANITA Note 04-002 [5]. In the past we have modeled the noise voltage in the simulations with a Gaussian distribution. Under this model, the probability f that the noise voltage will pass a threshold $V_{\rm th}$ an a given instant in time is given by:

$$f = 2 \cdot \frac{1}{\sqrt{2\pi}} \frac{1}{\sigma} \int_{V_{\rm th}}^{\infty} e^{-V^2/2\sigma^2} dV. \tag{4}$$

The 2 in front accounts for events on the negative tail of the distribution. If we now perform a change of variables $P = V^2/R$, $dP = (2V/R)dV$, then after a little algebra we get:

$$f = \frac{1}{\sqrt{2\pi}} \frac{\sqrt{R}}{\sigma} \int_{P_{\rm th}}^{\infty} \frac{1}{\sqrt{P}} e^{-PR/2\sigma^2} dP. \tag{5}$$

where $P_{\rm th} = V_{\rm th}^2/R$. Here the mean power is $\langle P \rangle = V_{\rm RMS}^2/R = \sigma^2/R$, and so this becomes:

$$f = \frac{1}{\sqrt{2\pi}} \frac{1}{\sqrt{\langle P \rangle}} \int_{P_{\rm th}}^{\infty} \frac{1}{\sqrt{P}} e^{-P/2\langle P \rangle} dP. \tag{6}$$

So, the power distribution is an exponential multiplied by a Jacobian, $1/\sqrt{P}$. Cutting on $V_{\rm th}$ in voltage gives you the same probability of passing as cutting on $P_{\rm th} = V_{\rm th}^2/R$ in power.

A.2 Envelopes of the Noise Voltage Follow a Rayleigh Distribution

Although instantaneous snapshots of noise should follow a Gaussian distribution, the envelope of the noise follows a Rayleigh distribution. Under a system that detects noise envelopes, the probability f that the noise envelope a will exceed a threshold a_{th} is given by Goodman (4.2-6) [2]:

$$f = \int_{a_{\rm th}}^{\infty} \frac{a}{\sigma^2} e^{-a^2/2\sigma^2} da. \tag{7}$$

In this case, this integral over amplitudes of voltage envelopes is in fact performed by substituting power envelope for voltage envelope, $I = a^2/R$:

$$f = \frac{R}{2\sigma^2} \int_{I_{\rm th}}^{\infty} e^{-IR/2\sigma^2} dI, \tag{8}$$

where $I_{\mathrm{th}} = a_{\mathrm{th}}^2/R$. This equation is the same as Goodman (4.2-7). Here the mean power envelope is $\langle I \rangle = 2\sigma^2/R = 2\langle P \rangle$ as in Goodman (4.2-8), and so this now becomes:

$$f = \frac{1}{\langle I \rangle} \int_{I_{\mathrm{th}}/\langle I \rangle}^{\infty} e^{-I/\langle I \rangle} dI, \tag{9}$$

which is Goodman (4.2-9). Evaluating the integral, we get

$$f = e^{-P_{\mathrm{th}}/\langle P \rangle} = e^{-a_{\mathrm{th}}^2/2\sigma^2}. \tag{10}$$

Notice that for noise amplitude that follows a Rayleigh distribution, envelope of the power does follow a pure exponential, as seen in Equation 9.

B Where the Formula in J. Middleditch's Thesis Comes From

Formula (45) in Middleditch's thesis [4] reads (in terms of the variables defined in the previous sections):

$$\frac{I_{\mathrm{th}}}{\langle I \rangle} \approx \frac{1}{2}\left(\frac{V_{\mathrm{th}}}{\sigma}\right)^2 + \ln\left(\sqrt{\frac{\pi}{2}} \cdot \frac{V_{\mathrm{th}}}{\sigma}\right). \tag{11}$$

This appears to come from equating:

$$\frac{1}{\langle I \rangle} \int_{I_{\mathrm{th}}}^{\infty} e^{-I/\langle I \rangle} dI = \frac{1}{\sqrt{2\pi}} \frac{1}{\sigma} \int_{V_{\mathrm{th}}}^{\infty} e^{-V^2/2\sigma^2} dV. \tag{12}$$

Using:

$$\mathrm{erfc(x)} = \frac{2}{\sqrt{\pi}} \int_{\mathrm{x}}^{\infty} \mathrm{e}^{-\mathrm{t}^2} \mathrm{dt} \tag{13}$$

Equation 12 becomes

$$e^{-I_{\mathrm{th}}/\langle I \rangle} = \mathrm{erfc}\left(\frac{\mathrm{V_{th}}}{\sqrt{2}\sigma}\right) \tag{14}$$

From Abramowitz & Stegun,

$$\sqrt{\pi} z e^{z^2} \mathrm{erfc(z)} \approx 1 + ... \tag{15}$$

and so substituting $z = V_{\mathrm{th}}/\sqrt{2}\sigma$ into Equation 15 and inserting into Equation 12 gives:

$$e^{-I_{\mathrm{th}}/\langle I \rangle} \approx \sqrt{\frac{2}{\pi}} \frac{\sigma}{V_{\mathrm{th}}} e^{-V_{\mathrm{th}}^2/2\sigma^2} \tag{16}$$

and if we take the natural log of both sides of Equation 16 we get Equation 11. The important thing to note is that Equation 12, on which all of this is based, seems to equate an integral over a pure exponential in power envelopes, as in the Rayleigh formalism (see

Equation 8), to an integral over a Gaussian in instantaneous voltages, as in Equation 4. Therefore, Equation 11 should be used with extreme caution since the two sides of the equation describe different types of detection systems.

If one is consistent with their choice of model for the noise voltage, whether it be Gaussian or Rayleigh, and perform a change of variables to power, the relationship between the cuts that one should make in the power domain and voltage domain to obtain the same singles rates should be $P_{\rm th} = V_{\rm th}^2/R$ or $I_{\rm th} = a_{\rm th}^2/R$.

Equation 11 would, however, be applicable if one were making measurements using an envelope detector in the lab and trying to find the corresponding cut in instantaneous voltage in a simulation that models measurements of noise with a Gaussian distribution. This was indeed the case at the time Note #4 was posted (if we assume that the power is measured by an envelope detector) and so it was appropriate to use a cut on voltage derived from the measured cut in power and Equation 11. In Note #4, the $V_{\rm th}/\sigma = 2.3$ came from a $I_{\rm th}/\langle I\rangle = 3.7$, satisfying Equation 11.

Now the simulations are moving from the Gaussian model to the Rayleigh/Rician model and so now, both the noise power measured in the lab and the models for noise voltage in the simulations are under the Rayleigh formalism, and so the relationship between the cuts in the power and voltage domains would be just $I_{\rm th} = a_{\rm th}^2/R$ if we had a true envelope detector. One has to be careful to remember that $\langle I\rangle = 2\sigma^2/R$ as in Goodman (4.2-8) when solving for $V_{\rm th}$ in Equation 11. For example, for a cut on a power envelope at $I_{\rm th}/\langle I\rangle = 3.7$, $a_{\rm th} = \sqrt{I_{\rm th}R} = \sqrt{3.7\cdot\langle I\rangle\cdot R} = \sqrt{2\cdot 3.7\cdot\sigma^2} = 2.7\sigma$.

For reference, we also derive the relationship between power relative to mean power envelope and a voltage envelope relative to σ:

$$\frac{I}{\langle I\rangle} = \frac{a^2/R}{2\sigma^2/R} = \frac{1}{2}\left(\frac{a}{\sigma}\right)^2 \tag{17}$$

C Comparing Numbers

For comparing numbers, we set R=1 for simplicity. Table 4 shows the probability for the noise voltage to pass the trigger at any given instant using Equation 4. Table 5 shows that one gets the same probabilities if one cuts on power instead of voltage, using simply $P_{\rm th} = V_{\rm th}^2/R$ and Equation 6.

Table 6 shows the probabilities that you would get if you were to cut on the instantaneous power using the equation from Middleditch's thesis, reproduced here as Equation 11, to find the threshold in power and using Equation 6 for the power distribution. Notice that the probabilities in Table 6 are not even a good approximation for those in Tables 4 and 5. This is because the proper relationship between cuts in instantaneous voltage and

instantaneous power are really $P_{\rm th} = V_{\rm th}^2/R$, not the Middleditch formula.

Table 7 shows the probability for the noise voltage envelope to pass the trigger at any given instant using Equation 7, now using the Rayleigh formalism. Table 8 shows that one gets the same probabilities if one cuts on power envelope instead of voltage envelope, using simply $I_{\rm th} = a_{\rm th}^2/R$ and Equation 8.

The numbers in bold in the tables correspond to the cut that we have been using in the simulations. A cut on instantaneous voltage at $V_{\rm th}/\sigma = 2.3$ using the Gaussian formalism (Table 4) is equivalent to a cut on $P_{\rm th} = V_{\rm th}^2/R = 5.3$ also using the Gaussian formalism and measuring instantaneous power (Table 5). Both give a probability of 2.14% of passing the cut for any instantaneous measurement.

If we move to the Rayleigh formalism for an envelope detector, then the equivalent cut on the power envelope is obtained from the Middleditch formula, Equation 11, giving a cut on the power envelope at $I_{\rm th} = \left[\frac{1}{2}\left(\frac{V_{\rm th}}{\sigma}\right)^2 + \ln\left(\sqrt{\frac{\pi}{2}} \cdot \frac{V_{\rm th}}{\sigma}\right)\right] \cdot \langle I \rangle = \left[2.3 * 2.3/2 + \ln\left(\sqrt{\pi/2} \cdot 2.3\right)\right] \cdot 2 = 7.4$ (see Table 8). Remember that this cut is $I_{\rm th}/\langle I \rangle = 3.7$, expressed as relative power of the envelope. The equivalent cut on the voltage envelope is given by $a_{\rm th} = \sqrt{I_{\rm th} R} = 2.7$ (see Table 7). These cuts give a probability of 2.5% of passing the cut of an envelope detection measurement. This is close to the 2.14% obtained from the Gaussian formalism, remembering that the Middleditch formula is an approximation.

The last row of each of the Tables follow this same procedure through for a higher cut (5 σ in the Gaussian formalism, 5.4 σ in the Rayleigh formalism) since the Middleditch formula should be an even better approximation in that region. There the probabilities are even closer (5.7E-5 compared to 5.9E-5).

D Conclusion

Since the power threshold levels $I_{\rm th}$ in Note #4 were set according to an exponential distribution in power envelopes, then it is indeed appropriate to use the Middleditch formula to obtain the equivalent cut in *instantaneous voltage* $V_{\rm th}$, under the Gaussian formalism. However, once the noise voltage measurement is modeled as envelope detection, then we use the Rayleigh distribution to model the noise voltage envelopes a and in that case the appropriate cut should be given by $a_{\rm th} = \sqrt{I_{\rm th} \cdot R}$.

So, for a cut on relative power at 3.7, the appropriate cut on instantaneous voltage was 2.3 using the Middleditch formula. However, once we move to the Rayleigh/ Rician formalism to model envelope detection of noise, the cut should increase to 2.7 to keep the same singles rate.

V_{th}/σ	f (%, Voltage Threshold from Equation 4)
2.0	4.55
2.3	**2.14**
3.0	0.27
5.0	5.73E-5

Table 4: *Probability for instantaneous noise voltage to pass a cut using Equation 4.*

V_{th}/σ	$P_{\mathrm{th}}/\langle P\rangle$	$P_{\mathrm{th}} = V_{\mathrm{th}}^2/R$	f (%, Power Threshold from Equation 6)
2.0	4.0	4.0	4.55
2.3	**5.3**	**5.3**	**2.14**
3.0	9.0	9.0	0.27
5.0	25.0	25.0	5.73E-5

Table 5: *Probability for instantaneous noise power to pass a cut using Equation 6.*

V_{th}/σ	$P_{\mathrm{th}}/\langle P\rangle$	$P_{\mathrm{th}} = \left[\frac{1}{2}\left(\frac{V_{\mathrm{th}}}{\sigma}\right)^2 + \ln\left(\sqrt{\frac{\pi}{2}}\cdot\frac{V_{\mathrm{th}}}{\sigma}\right)\right]\cdot\langle P\rangle$	f (%, Power Threshold from Equation 11)
2.0	2.9	5.8	8.75
2.3	**3.7**	**7.4**	**5.43**
3.0	5.8	11.6	1.58
5.0	14.3	28.7	1.53E-2

Table 6: *Probability for instantaneous noise power to pass a cut using Equation 11.*

a_{th}/σ	f (%, Voltage Threshold from Equation 7)
2.0	13.5
2.3	7.10
2.72	**2.46**
3.0	1.11
5.0	3.73E-4
5.35	5.95E-5

Table 7: *Probability for a noise voltage envelope to pass a cut using Equation 7. The numbers in bold show the cut on noise voltage envelope that is equivalent to a cut on instantaneous noise voltage at 2.3.*

$a_{\rm th}/\sigma$	$I_{\rm th}/\langle I\rangle$	$I_{\rm th} = a_{\rm th}^2/R$	f (%, Power threshold from Equation 8)
2.0	2.0	4.0	13.5
2.3	2.6	5.3	7.10
2.72	**3.7**	**7.4**	**2.46**
3.0	4.5	9.0	1.11
5.0	12.5	25.0	3.73E-4
5.35	14.3	28.7	5.95E-5

Table 8: *Probability for a noise power envelope to pass a cut using Equation 8.*

References

[1] P. Gorham, ANITA Note 68.

[2] J. Goodman, "Statistical Optics," 1985.

[3] M. Schwartz, "Information Transmission Modulation and Noise," 1959.

[4] J. Middleditch, Ph.D. thesis, unpublished. Gary Varner faxed me two pages of the thesis, the one containing Equations 45-47 and the preceding page.

[5] Varner *et al.*, ANITA Note 04-002.